Article

Not peer-reviewed version

A New Approach to Non-Invasive Microcirculation Monitoring: Quantifying Capillary Refill Time Using Oximetric Pulse Waves

Yuxiang Xia , Xinrui Wang , Zhe Guo , Xuesong Wang * , Zhong Wang *

Posted Date: 7 November 2024

doi: 10.20944/preprints202411.0568.v1

Keywords: microcirculation; capillary refill time; oxygen pulse wave; sepsis; non-invasive monitoring

Article

A New Approach to Non-Invasive Microcirculation Monitoring: Quantifying Capillary Refill Time Using Oximetric Pulse Waves

Yuxiang Xia [1], Xinrui Wang [1], Zhe Guo [1,2], Xuesong Wang [1,2,*] and Zhong Wang [1,2*]

[1] School of Clinical Medicine, Tsinghua University, Beijing, China, 30 Shuangqing Road, Haidian District Beijing, Beijing, 102218, China
[2] Beijing Tsinghua Changgeng Hospital Affiliated to Tsinghua University, Beijing, China, 168 Litang Road, Changping District, Beijing, 102218, China
* Correspondence: chenjiu0525@163.com

Abstract: (1) Background: A new type of capillary refill time measurement system is proposed to be designed to achieve non-invasive, mechanised and standardised measurement of the microcirculatory status of the human body; (2) Methods: First, a mechanical measurement device based on electromagnetic pressurisation technology was designed for the measurement of microcirculation monitoring indexes such as capillary refill time, and the measurement control logic was set based on clinical application scenarios; second, the haemoglobin content in the arterial blood flow in the distal capillary bed was continuously monitored, and a software system was designed for the automatic acquisition, transmission, analysis, computation, and storage of the raw data and noise removal algorithms were proposed for the mutational noise present in the data; finally, healthy adult subjects were recruited to carry out a preliminary clinical observational study to evaluate the reproducibility and reliability of the measured parameters; (3) Results: A capillary refill time meter test machine was developed with good CRT reproducibility, both between different observers and between different numbers of observations for a uniform observer; (4) Conclusions: Rapid non-invasive monitoring of microcirculation has been successfully achieved, making non-invasive monitoring of microcirculation further mechanised and standardised, with the advantages of simple measurement and high accuracy..

Keywords: microcirculation; capillary refill time; oxygen pulse wave; sepsis; non-invasive monitoring

1. Introduction

In recent years, with the continuous development of haemodynamic theory and the continuous progress of clinical monitoring technology, the problem of the decoupling of the macrocirculation and microcirculation has become a hotspot of concern for clinical researchers. For many critically ill patients, the stabilisation of the macrocirculation may only be the first step in the treatment process, while the improvement of microcirculation is the key to the treatment of critically ill patients [1–4]. At present, in the diagnosis and treatment of critically ill patients, microcirculatory status is commonly measured by blood lactate, central venous oxygen saturation (ScvO2), central venous-to-arterial carbon dioxide gap (CO2-gap), and other respiratory oxygen metabolism parameters. -gap) and other respiratory oxygen metabolism indicators to indirectly infer, but these invasive indicators are easily affected by respiratory function abnormalities, metabolic function abnormalities, measurement errors and other factors, how to intuitively and real-time monitoring of microcirculation status has received more and more attention, but the tricky thing is that the microcirculation status of the patient's deep organs is difficult to be directly monitored in practice. Intuitive and accurate peripheral circulation monitoring techniques are urgently needed to help improve the current situation of tissue perfusion monitoring in critically ill patients.

Capillary Refill Time (CRT), as the most intuitive monitoring index of peripheral circulatory blood flow status, has been widely used in various aspects such as condition judgement, treatment guidance and prognosis evaluation of critically ill patients due to the advantages of being intuitive,

 doi:10.20944/preprints202411.0568.v1

convenient and non-invasive [5–13]. Patients resuscitated with CRT normalisation as the resuscitation goal have less organ dysfunction at 72h, less intravenous rehydration and lower 28-day mortality [11]. Currently, the International Sepsis Guidelines, the American Academy of Paediatrics, the World Health Organization and the American Heart Association all recommend the inclusion of CRT measurements as an important part of systematic assessment [14–17]. In order to obtain accurate and reliable quantitative data, we have developed a capillary refill time meter test machine by applying internet thinking and artificial intelligence technologies such as deep learning to achieve fully automated and non-invasive measurement of microcirculation.

2. Materials and Methods

2.1. Detection Principles

Capillary refill time is measured artificially by pressing the peripheral skin tissues of the body so that local blood flow is interrupted, blood is squeezed to the periphery, skin discolouration occurs, local blood flow is gradually restored after removal of the pressure, and the time taken for the nail beds or the skin to become flushed red again is recorded. Therefore, automatic measurement of capillary refill time requires automatic compression and instantaneous release of peripheral skin and continuous monitoring of changes in distal tissue blood flow during this process.

According to the Lambert-Beer law [18], when the ventral surface of the distal phalanx of the right index finger is vertically irradiated using continuous parallel single-wavelength NIR light, the amount of absorbed light is directly proportional to the thickness of the irradiated tissue and the concentration of haemoglobin (oxyhaemoglobin + reduced haemoglobin). As shown in equation (1), when the amount of incident light I0 is constant, the tissue thickness B is constant, and the molar absorption coefficients of haemoglobin for 900 nm near-infrared light, K_{HbO2} and K_{Hb}, are constant, then the amount of transmitted light received, I, can reflect the change in the concentration of haemoglobin (oxygenated haemoglobin + reduced haemoglobin) in the blood flow, C_{HbO2} and C_{Hb}. When the blood flow at the end of the finger changes, the C_{HbO2} and C_{Hb} in the capillary bed will also change, and the transmitted light quantity I will also change in synchrony with the blood flow at the end of the finger.

$$A = \lg\left(\frac{I_0}{I}\right) = (K_{Hbo2}C_{Hbo2} + K_{Hb}C_{Hb}) \times B \quad (1)$$

On this basis, we simultaneously designed an electromagnet pressurisation device to achieve pressurisation and instantaneous release of the finger end. When the end of the finger is pressurised, the tissue is squeezed, arterial blood flow stops and the beat wave signal disappears; venous and capillary blood flow decreases, haemoglobin (oxyhaemoglobin + reduced haemoglobin) concentration decreases, the tissue thickness is relatively reduced, the amount of absorbed light decreases, and the amount of transmitted light increases, and the non-beat signal detected by the sensor is enhanced. When the pressurising device releases the pressure, the tissue thickness increases, the concentration of haemoglobin (oxygenated haemoglobin + reduced haemoglobin) gradually recovers, the amount of absorbed light increases, the amount of transmitted light decreases, the non-pulsating pulsatile wave signals detected by the sensor gradually fall back, and pulsatile wave signals gradually recover with the restoration of the arterial blood flow, and we consider that, when the transmissible photoelectric signals detected by the sensor recover to the baseline level before the pressurising device refilling of the peripheral vasculature was achieved (Figure 1).

Preprints.org (www.preprints.org) | NOT PEER-REVIEWED | Posted: 7 November 2024 doi:10.20944/preprints202411.0568.v1

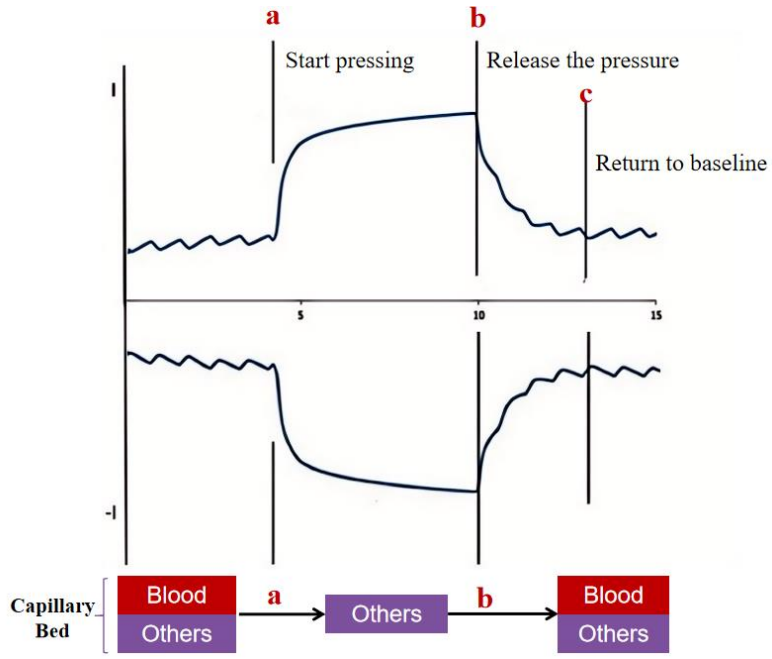

Figure 1. Schematic diagram of instrumented measurement of capillary refill time.

2.2. Design and Implementation of Instrumented Measurement of Capillary Refill Time

Figure 2 shows a schematic of a mechanised CRT measurement, where a press actuator acts on the finger to affect the blood content in the terminal capillary bed, resulting in a change in blood oxygen concentration (Figure 2A). The blood oxygen concentration is expressed via a PPG, which is flipped to form a discrete time series (Fig. 2B), with each element of the sequence consisting of the sampling time ti and the corresponding blood oxygen value x(t_i):CRT = $\{(t_i, x(t_i)|i = 1,2\ldots N)\}$.The current instrument samples the optoelectronic signal at a frequency of *f*=50Hz, and usually a complete CRT test consists of five phases from Δt_0-$\Delta t_4$with an overall time of about 15s.

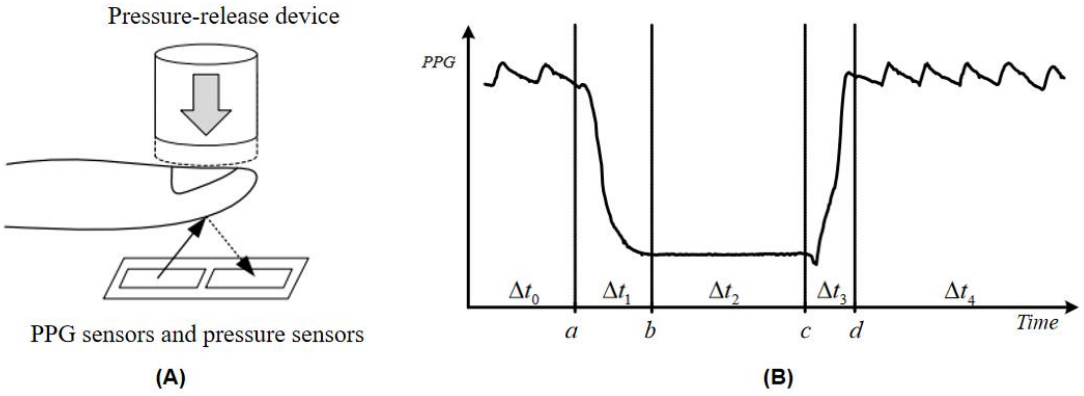

Figure 2. (A) Electromagnet-based press-release device. capable of instant rebound after power failure, it does not interfere with blood return as compared to other mechanical compression devices. PPG sensors are able to continuously monitor the amount of light reflected from the end of the finger, and pressure sensors monitor the amount of pressure in real time.(B) PPG signal curve. The regular undulation with the heart beat is called the baseline state, when the instrument automatically detects the baseline state for a period of time, the pressing device starts to apply pressure to the finger, and this period of time is recorded as Δt_0; with the gradual increase of the pressure, the arterial blood in the capillary bed is gradually drained, and the concentration of hemoglobin drops sharply, which is reflected in the figure as a section of the PPG signal curve that decreases rapidly, and the PPG signal curve decreases rapidly when it reaches a certain pressure threshold value (3-5N) is reached, the pressure device stops increasing the pressure, and this period of time is recorded as Δt_1;Since the end of the finger is essentially emptied of blood, it is reflected in the figure as a segment of the PPG signal curve that is essentially free of fluctuations, and the period of time during which the signal remains steady at a low level is

 doi:10.20944/preprints202411.0568.v1

noted as Δt_2;The electromagnet is released instantaneously, the blood in the capillaries at the end of the finger gradually fills up, and the blood circulation and hemoglobin concentration will return to pre-pressure levels for a period of time noted as Δt_3;After the PPG signal curve returns to a stable fluctuation, it is then continued to be observed for a period of time as a sign of a successful test, which is noted as $\Delta t4$;a: initiation of compression; b: maintenance of compression; c: release of pressure; d: return of blood to return to baseline status.

The Capillary Refill Time Measuring Instrument is mainly composed of a PPG sensor module, a pressure sensor, a power actuator module, a lithium battery pack, a microcontroller and its control circuit, an emergency release device, a scanning port for the wristband, and a high-definition display (Figure 3). Compared with the existing measuring instruments, this instrument has the following advantages: compact size, easy to use in emergency departments and outpatient wards; unique electromagnetic design makes the pressure device can instantly rebound, thus ensuring that the measurement results are true and reliable; the addition of wristband scanning port: scanning the patient's wristband to automatically import the information of the test subject and storage of the test results, which is easy to use in the clinic; uniquely designed emergency release device, the pressure can be released and stop the measurement at any time, which ensures the reliability and reliability of the measurement results. Uniquely designed emergency release device, release the pressure at any time during the measurement process, stop the measurement, to ensure the safety of the instrument; visualisation window design, the measurer and the subject can intuitively see the finger placement position and timely adjustments to improve the success rate of the measurement; ergonomic design to fit the hand shape, so that the hand is relaxed and comfortable, to avoid measurement errors caused by the stiffness of the hand.

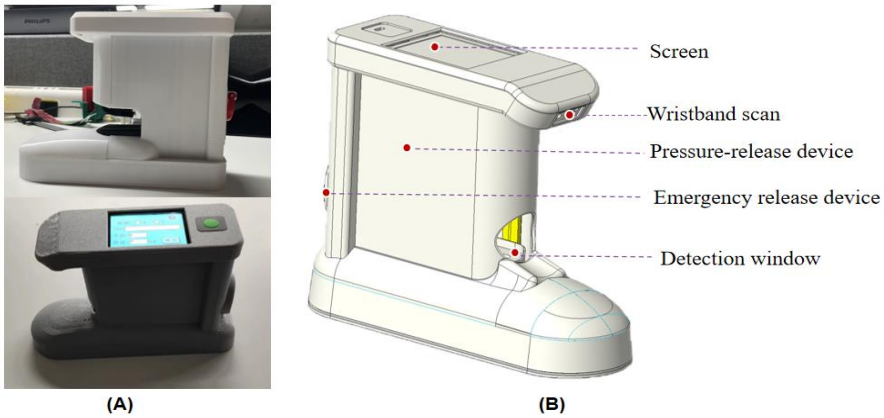

Figure 3. (A) Photograph of the portable capillary refill time meter; (B) 3D view of the capillary refill time meter.

We set up the measurement control logic for the instrumentation of capillary refill time based on the clinical application scenario, and set the pressure of the machine on the finger to be automatically controlled by the software, stopping the pressure when the detected waveform of the electrical signal is a straight line, and releasing the pressure automatically after it has been maintained for 5 s, which is equivalent to the pressing time of the finger using the final pressure of 5 s. It is important to note that a stable pulse waveform needs to be obtained before the start of the measurement to determine the baseline position. graph to determine the baseline position. Data recording began with the recording of a stable pulse wave pattern 5 s before compression and continued until 10 s after the end of compression to ensure that the recorded blood flow refill curve returned to the baseline position. In addition, considering the safety of clinical use, protection control is set up so that the power supply can be cut off at any time during the whole measurement process, and compression can be stopped at any time during compression through the ‘emergency release device’, and the compression pressure can be released at any time, according to the clinical use scenarios set up in the control logic diagram shown in Fig. 4.

Preprints.org (www.preprints.org) | NOT PEER-REVIEWED | Posted: 7 November 2024 doi:10.20944/preprints202411.0568.v1

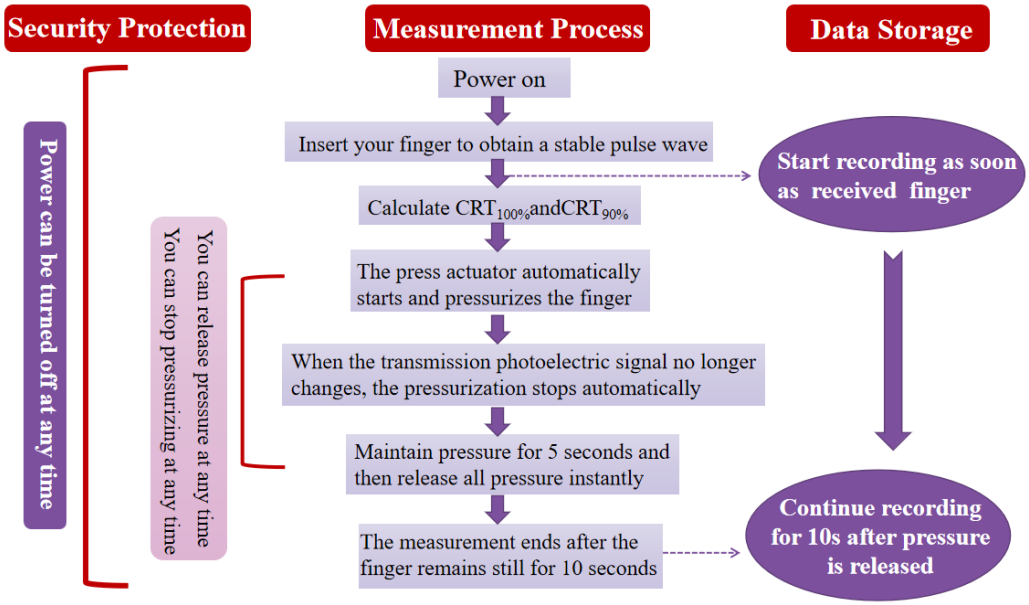

Figure 4. Control Logic Diagram of Capillary Refill Time Measuring Instrument Tester.

2.3. Design and Realisation of an Automated Processing System for Blood Oxygen Measurement Data

2.3.1. Removal of Mutant Noise

In the process of analysing and processing the blood oxygen measurement data, we found that, under the influence of the photoelectric sensor, there is often a sudden change in the data (as shown in Fig. 5), which appears randomly and has no fixed frequency, and when it appears, it completely masks the original signal value, which belongs to the other noises in the fourth type mentioned above, and it is impossible to remove them by using the traditional filtering methods. At the same time, this type of noise can cause serious interference to the signal calculation results, such as causing the peaks and valleys detection algorithm to fail, which in turn leads to measurement failure. Define (Pa, Pb, Pc, Pd) to denote the four stages of the mutation noise, the beginning of the mutation, the mutation recovery, and the end of the mutation, respectively, and the corresponding instantaneous slopes of the four points (as Ka, Kb, Kc, Kd), respectively. Among them, if downward mutation noise occurs, the corresponding instantaneous slopes of the signals will, in general, reflect the characteristic of 'down (Ka-Kb)-up (Kb-Kc)-down (Kc-Kd)' in the lower right of Fig. 6(A); if upward mutation noise occurs, the corresponding instantaneous slopes will reflect the characteristic of 'up-down-up (Kc-Kd)' in the lower left of Fig. 6(A); and if upward mutation noise occurs, the corresponding instantaneous slopes will reflect the characteristic of 'up-down-down-up (Kc-Kd)' in the lower left of Fig. 6(A). 'up-down-up' feature in the lower left of Fig. 6(A). When continuous mutation in time and long duration mutation occurs, there will be more than one mutation point appearing, at which time the mutation point Pb becomes a collection including (Pb1, Pb2, Pb3) and so on appearing in it.

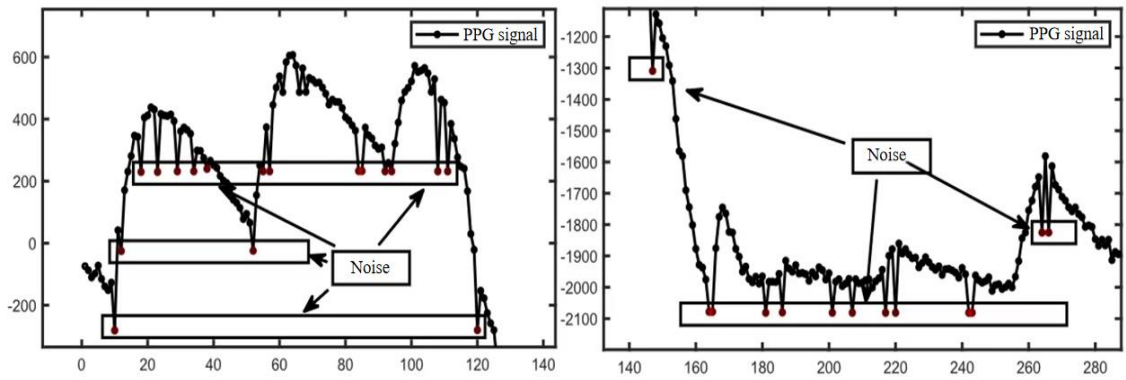

Figure 5. Schematic diagram of mutation noise.

Preprints.org (www.preprints.org) | NOT PEER-REVIEWED | Posted: 7 November 2024 doi:10.20944/preprints202411.0568.v1

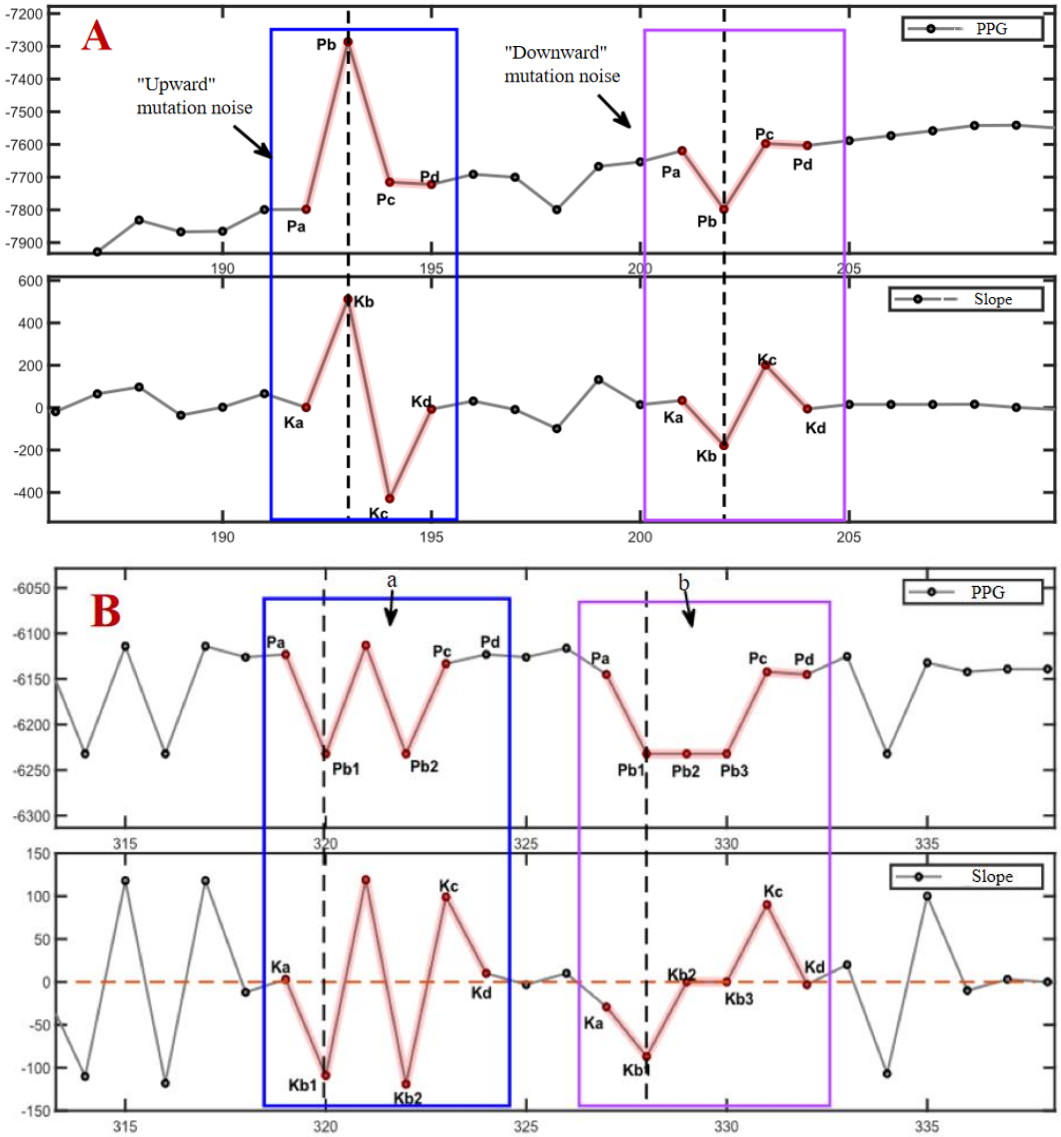

Figure 6. Classification of mutation noise. The upper vertical coordinate is the oximetry data (PPG), and the lower graph shows the corresponding instantaneous slope of the signal. Figure 6(A) shows a schematic diagram of "upward" and "downward" mutation noise, and Figure 6(B) shows a schematic diagram of continuous and sustained mutation noise, where a denotes continuous mutation noise and b denotes sustained mutation noise.

According to the different directions in the amplitude when it occurs, the noise can be classified into upward mutation and downward mutation, and this kind of noise can be further classified into three kinds according to the continuity in time: a single occurrence, a number of consecutive occurrences, and a long period of time continually occurring (shown in Fig. 5). After a mutation noise, followed by a mutation noise, if the first-order difference between *Kb2* and *Kb3* set a point equivalent to the level of *Ka*, i.e., the first and last of the two single mutation first-order difference features 'down-up-down'. The situation where the mutation noise occurs and is not recovered for a continuous period of time is called long lasting mutation noise, as shown on the right side of Fig. 6. According to the statistical analysis, when this situation occurs, the signal value will remain unchanged at the mutation position, i.e., *Pb1=Pb2=Pb3*, etc., and therefore, the corresponding first-order difference value also remains unchanged and equals to zero, i.e., *Kb2=Kb3=0*.

Taking full consideration of the characteristics of the noise itself, we propose the idea of utilizing four-point slope features to locate the noise and remove it. The whole noise process is divided into four processes: start, mutation, mutation recovery, and end, and the key points of these four processes

 doi:10.20944/preprints202411.0568.v1

are identified in the signal by first-order difference. The instantaneous slope values were approximated by calculating the first-order difference of the oximetry data using the formula as shown in equation (2) below.

$$x'(t_i) = \frac{x(t_i) - x(t_{i-1})}{t_i - t_{i-1}}, i = 2,3,\ldots,N \quad (2)$$

According to the described time domain morphological features, the algorithm is designed to determine whether a noise point is suspicious by using the magnitude and direction of the change of the instantaneous slope. If the instantaneous slopes $x'(t_i)$ and $x'(t_{i-1})$ corresponding to a point t_i and its previous point t_{i-1} satisfy the relationship described in equation (3), the current signal point is considered suspicious.$\triangle x'$ as a slope threshold, which can be set as an observation or as a variance of the instantaneous slope close to Pb for a period of time, the threshold can be used to regulate the sensitivity of the algorithm, and the larger the threshold, the less sensitive the algorithm is to small magnitude mutant noise. Further the found suspicious noise point is noted as Pb. Subsequently further search for related points Pa, Pc, and Pd is required, and if all are matched successfully, then Pb is recognized as mutant noise. The matching process needs to take into account both continuous and persistent situations to finalize the removal of the noise.

$$|x'(t_i) - x'(t_{i-1})| > \triangle x' \text{ and } x'(t_i) \times x'(t_{i-1}) < 0 \quad (3)$$

2.3.2. Calculation of Pressure Release Recognition Points

The pressure release point is the point in time when the pressure is maintained for a period of time and then suddenly released. Prior to this point, the hemoglobin level in the blood remains stable at a low level due to the continuous maintenance of pressure, and after the pressure release point, the oxygen level in the blood rises rapidly due to the refilling of the capillaries and then returns to the baseline level, with the overall characteristic of "level-rapidly rising". The overall characteristic of "level-rapid rise", so as long as the blood oxygen measurement data to locate such a section of the characteristics, you can find the pressure release point. In practice, however, the fluctuation of the sensitivity of the device and the presence of mutation noise make the implementation of the feature recognition algorithm based on the raw data more complicated. The identification of the press-release point seems to be more concerned with the overall trend of the signal, so we propose the quadratic Exponentially Weighted Averages-K (EWAK) algorithm. Exponentially Weighted Averages (EWA) were firstly applied to the PPG data to remove some of the high frequency and mutation noise effects while flattening the signal, based on which the corresponding instantaneous slopes of the signals were calculated using Eq. (4), and finally the exponentially weighted averages were used again to finally get the smoother *EWAK* curve as the approximate first-order derivative curve of the PPG. Among them, the calculation of exponentially weighted average can effectively reduce the influence of high-frequency information in the signal and facilitate the observation of the overall trend, and the EWA calculation formula is as follows:

$$EWA(t_i) = \beta \times EWA(t_{i-1}) + (1-\beta) \times x(t_i), \beta \in [0,1) \quad (4)$$

$EWA(t_i)$ as an estimate of moment t_i, which can be substituted for the actual observation at this moment and is approximately equal to the average of the actual observations in the past $1/(1-\beta)$ moments, where indicates the weight of the data in the past period, which is an adjustable parameter, where larger values indicate that more past data are used, and smaller values indicate that the data at the current moment have a greater weight. When $\beta = 0.9$, $EWA(t_i)$ is approximately the average of the last 10 values. However, setting β too large means that more past data are used, which will cause a significant signal hysteresis that may result in points being recognized later than when they really occurred.

The instantaneous slopes are computed to approximate the first-order derivatives, and their peak points serve as the basis for critical point identification. A segment of the PPG signal is represented using a straight line, and the computed EWAK curve is represented using a dashed line. An example of the comparison of the PPG signal with the corresponding quadratic sliding average-derivative values is shown in Figure 7. The EWAK curve corresponding to the oximetry data near the point of pressure release shows a steady characteristic, i.e., it rises rapidly after a nearly horizontal

 doi:10.20944/preprints202411.0568.v1

curve and reaches the maximum point of the whole curve, as shown in the figure using the red highlights. The EWAK curve approximates a first-order derivative, and the maximum point means the point of maximum velocity in the oximetry data, which corresponds to the fastest point in capillary filling in the real sense. phase. Therefore, the algorithm starts from the maximum point and looks for such a smooth curve to the left, and at the transition between the smooth curve and the rising curve, the corresponding point in the oximetry data is the point to be searched for the pressure release point, as shown by the intersection of the vertical dashed line and the PPG signal in the figure.

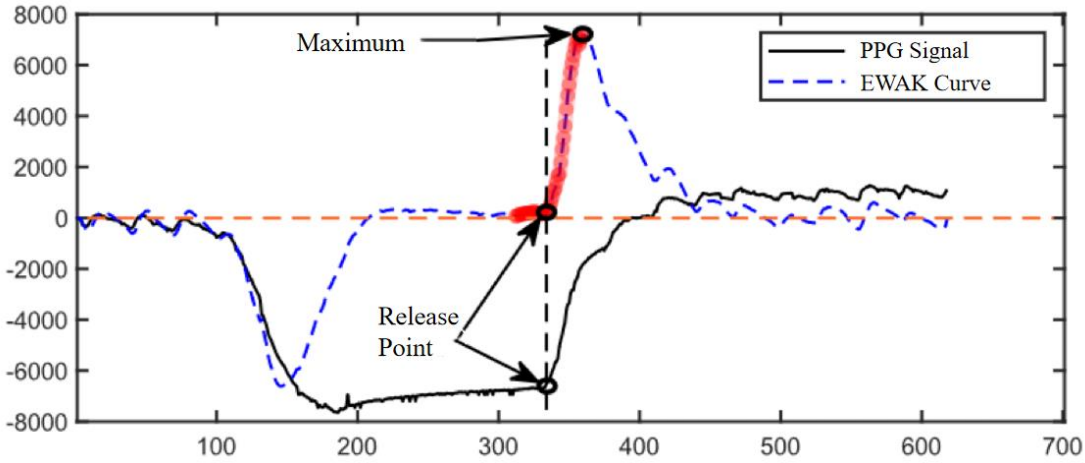

Figure 7. CRT data and its EWAK curve.

2.4. Reliability and Reproducibility of This Device for Assessing Capillary Refill Time

This study was a prospective single-center observational study in which 10 healthy adult subjects were recruited at Tsinghua University. Inclusion criteria: healthy adults, age ≥18 years, no previous serious organ dysfunction or peripheral vascular disease. Exclusion criteria: diabetes mellitus; hypertension; systemic vasculitis; upper extremity arterial occlusion; upper extremity arterial thrombosis; pregnant or breastfeeding women; gray nails, nail polish, or thick nail beds that prevented the machine from obtaining valid data; and the absence of the right index finger prevented measurement. Subjects signed an informed consent form after understanding the contents of the experiment.

Two trained measurers (Measurement A, Measurement B) measured the right index finger of healthy subjects using a capillary refill time meter; Measurement A took one measurement and Measurement B took two measurements, each 5 minutes apart. Measurement to ensure that the ambient temperature is between 20-25 °C, the subject stays in the environment for more than 30 min, the fingertip is raised to a position roughly the same height as the heart and put into the detection window according to the prompts, the instrument acquires a stable pulse wave pattern and then automatically presses down, stops pressing when the detected electrical signal waveform is a straight line, the pressure is maintained for 5 s and then automatically released, and continues to be recorded until 10 s after the end of the compression, in order to Ensure that the recorded blood flow refill curve returns to the baseline position. Three values are obtained at the end of a measurement for reference: CRT_k indicates the CRT value calculated using the slope of the curve after the release of the pressure as the core, $CRT_{100\%}$ indicates the time elapsed from the point of release of the press to the intersection of the pulse wave and the baseline, and $CRT_{90\%}$ indicates the time elapsed from the point of release of the press to the intersection of the pulse wave and the 90% baseline.

3. Results and Discussion

3.1. Testing of Automated Systems for Processing Oximetry Data

In order to evaluate the denoising effect of the algorithm on mutant noise, a common metric for measuring the difference between values is used, namely, root mean square error (RMSE), which is

Preprints.org (www.preprints.org) | NOT PEER-REVIEWED | Posted: 7 November 2024 doi:10.20944/preprints202411.0568.v1

commonly used in the field of signal processing to evaluate the difference between the real signal without noise and the filtered and denoised signal, with smaller values indicating better filtering. The RMSE calculation formula is shown in (5). In the formula *N* denotes the length of the signal, CRT_r denotes the signal that does not contain mutation noise, and CRT_{de} denotes the signal that has been processed by the denoising algorithm.The overall evaluation process was (1) construction of CRT_r; (2) construction of random mutation noise *Noise*;(3) Random mutation noise *Noise* is added to CRT_r to obtain the oximetry data CRT_{sim};(4)Process CRT_{sim} using the mutation noise removal algorithm to obtain CRT_{de};(5)The effectiveness of the algorithm is evaluated using *RMSE* for CRT_r and CRT_{de}.

$$\mathrm{RMSE} = \sqrt{\frac{1}{N}\left[\sum_{k=1}^{N}\left(CRT_r(k) - CRT_{de}(k)\right)^2\right]} \tag{5}$$

The single oximetry data processed by this system is in the form of a discrete time series, where each element of the series consists of the sampling time t_i and the corresponding PPG value,$CRT = \{(t_i, x(t_i)|i = 1,2\ldots N)\}$.A CRT test with a total duration of $T = 15s$, and a sampling frequency of $F = 50Hz$, we can get $N = T \times F = 750$, and the number of mutations in Noise is 34.Using this algorithm for 40 manually created CRT_r and calculating the average RMSE, the minimum RMSE = 119.3 is obtained when the slope threshold $\Delta x' = 100$ is set.Applied on oximetry data, an example of the algorithm denoising effect is shown in Figure 8.Figure 8(A) intercepted from a section of the CRT test process when the signal is continuously pressed, the significance of this section of noise elimination is that it can make the accuracy of the subsequent keypoint identification algorithm effectively improved, because the algorithm needs to calculate the average variance of the signal over a period of time, and if too much mutation noise exists, it will have a serious impact on the average variance. Fig. 8(B) Intercept from a segment of the signal at baseline during the CRT test, when the signal regularly produces variations in response to heartbeats. The significance of this noise removal is that it allows the accuracy of the subsequent peak point identification algorithm to be effectively improved, as the algorithm relies on the identification of poles within a region, which can easily overwrite the poles in the normal signal if an abrupt change occurs.

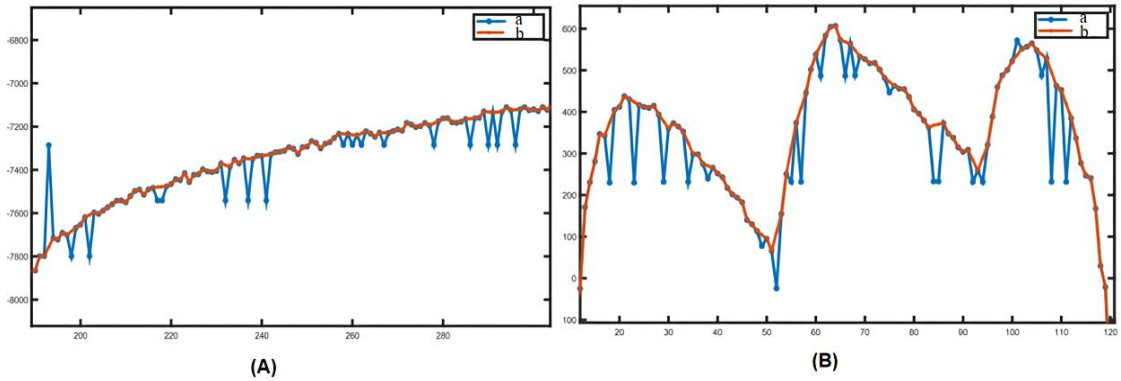

Figure 8. Example of denoising effect of this algorithm. In the figure, a represents the initial value of CRT and b is the CRT after removing the noise.

3.2. Reliability and Reproducibility of This Device to Assess Capillary Refill Time

A total of 10 healthy adult subjects meeting the inclusion criteria with a mean age of 61.4±14.9 years were included in this study, including 5 males and 5 females. The CRT values measured by Doctor A, Doctor B 1st and Doctor B 2nd were all in accordance with normal distribution, and none of the differences between them were statistically significant, with P greater than 0.05 (Table 1, Figure 9).

Table 1. *CRT_k*, *$CRT_{100\%}$*, *$CRT_{90\%}$* measured by two doctors.

Doctors	CRT_k*	$CRT_{100\%}$*	$CRT_{90\%}$*

 doi:10.20944/preprints202411.0568.v1

Doctor-A	1344.5±464.92	1217.3±560.3	1071.8±318.7
Doctor-B			
First measurement	1410.0±311.54	1100.9±286.7	1036.4±231.8
Second measurement	1385.5±185.06	1066.4±224.2	1011.8±183.7

* Variables in the table are expressed as (mean±SD).All CRT values are in milliseconds.

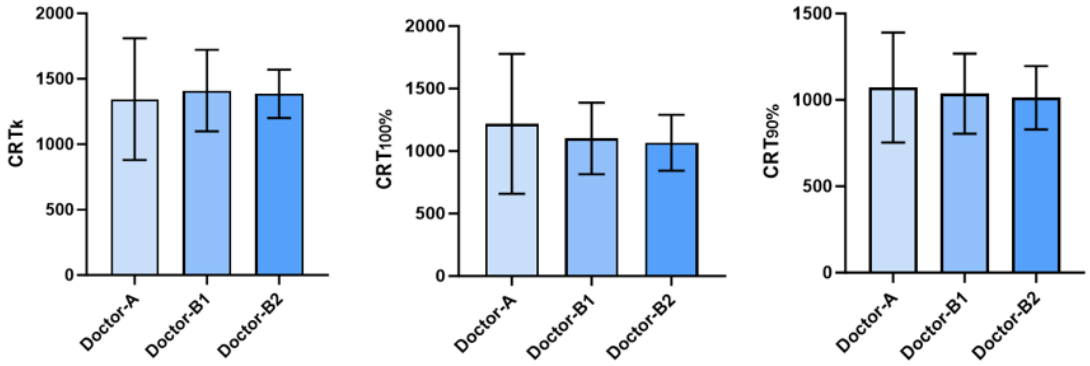

Figure 9. Comparison of CRTk, CRT100%, and CRT90% measured by two measurers.

4. Conclusions

When circulatory dysfunction occurs in the organism, peripheral circulation is often sacrificed the earliest to ensure blood perfusion of important organs; when circulatory function is gradually restored, it is restored the latest. Therefore, peripheral circulation monitoring indexes can sensitively reflect the status of systemic microcirculation blood flow. Based on the working mechanism of peripheral oxygen saturation monitoring technology commonly used in clinical practice, we searched for a method to continuously monitor fingertip blood flow, proposed a basic design for instrumentation to measure the indexes related to capillary refill time, and improved the existing equipment for the deficiencies in the control of compression time and force, the mechanism of determining the individualized capillary closure time, and the design of the compression actuating device. This system can instrument and standardize the measurement of the parameters related to capillary refill time, minimize the measurement error, improve the reliability and accuracy of the clinical index of capillary refill time, and the measurement process is non-invasive and simple. Preliminary clinical studies have shown that the measurement is stable and has good practical value and application prospects, providing a new idea for peripheral circulation monitoring.

5. Patents

We have applied for three invention patents, all of which have been disclosed and are currently under substantive examination. (Application Nos. 202410514816X, 2024106642551, 2024107379296)

Author Contributions: Conceptualization, YX Xia and Z Wang; methodology, YX Xia and XR Wang;Formal analysis, XS Wang and Z Wang; investigation, XR Wang;Data curation,XR Wang;writing—original draft preparation, YX Xia; writing—review and editing, XS Wang ,Z Guo and Z Wang;Project administration,Z Guo;funding acquisition, XS Wang.All authors have read and agreed to the published version of the manuscript.

Funding: This article is supported by Toyota Interdisciplinary Project 2022, Chronic Disease Management and Emergency Response Based on Tsinghua Healthcare Intelligent System (THIS) (Funding number: 20223930050), and Postdoctoral Fellowship Program of China Postdoctoral Science Foundation (Grant Number GZC20231341). The authors have no other relevant affiliations or financial involvement with any organization or entity with a financial interest in or financial conflict with the subject matter or materials discussed in the manuscript apart from those disclosed.

 doi:10.20944/preprints202411.0568.v1

Institutional Review Board Statement: The study was conducted in accordance with the Declaration of Helsinki, and approved by the Institutional Review Board (or Ethics Committee) of Beijing Tsinghua Changgeng Hospital Affiliated to Tsinghua University (protocol code 24033-4-01 and date of 2024-02-07).

Informed Consent Statement: Informed consent was obtained from all subjects involved in the study. Written informed consent has been obtained from the patient(s) to publish this paper" if applicable.

Data Availability Statement: The datasets used and/or analyzed during the current study are available from the corresponding author on reasonable request.

Conflicts of Interest: The authors declare no conflicts of interest.

References

1. Bakker J, Ince C. Monitoring coherence between the macro and microcirculation in septic shock.Curr Opin Crit Care.2020 NaN;26(3):267–272.
2. Ince C. Hemodynamic coherence and the rationale for monitoring the microcirculation. Crit Care.2015;19 Suppl 3(3):S8. doi:10.1186/cc14726.
3. Merdji H, Curtiaud A, Aheto A, et al. Performance of Early Capillary Refill Time Measurement on Outcomes in Cardiogenic Shock: An Observational, Prospective Multicentric Study.Am J Respir Crit Care Med. 2022;206(10):1230-1238. doi:10.1164/rccm.202204-0687OC.
4. Bodolea C. The Role of Microcirculation in Haemodynamics: A Journey from Atlas to Sisyphus.J Crit Care Med (Targu Mures). 2024;10(2):115-118. Published 2024 Apr 30. doi:10.2478/jccm-2024-0021.
5. Kattan E, Ibarra-Estrada M, Ospina-Tascón G, Hernández G (2023) Perspectives on peripheral perfusion assessment. Curr Opin Crit Care 29:208–214.
6. Hariri G, Joffre J, Leblanc G et al (2019) Narrative review: clinical assessment of peripheral tissue perfusion in septic shock. Ann Intensive Care 9:37.
7. Contreras R, Hernández G, Valenzuela ED et al (2022) Exploring the relationship between capillary refill time, skin blood flow and microcirculatory reactivity during early resuscitation of patients with septic shock: a pilot study. J Clin Monit Comput.
8. Brunauer A, Koköfer A, Bataar O et al (2016) Changes in peripheral perfusion relate to visceral organ perfusion in early septic shock: A pilot study. J Crit Care 35:105–109.
9. Lara B, Enberg L, Ortega M et al (2017) Capillary refill time during fluid resuscitation in patients with sepsis-related hyperlactatemia at the emergency department is related to mortality. PLoS ONE 12:e0188548.
10. Zampieri FG, Damiani LP, Bakker J et al (2020) Effects of a resuscitation strategy targeting peripheral perfusion status versus serum lactate levels among patients with septic shock. A Bayesian reanalysis of the ANDROMEDA-SHOCK trial. Am J Respir Crit Care Med 201:423–429.
11. Hernandez G, Ospina-Tascon G, Damiani LP et al (2019) Effect of a resuscitation strategy targeting peripheral perfusion status vs serum lactate levels on 28-day mortality among patients with septic shock. Andromeda-Shock Randomiz Clin Trial JAMA 321:654–664.
12. Kattan E, Hernández G, Tascón GO et al (2020) A lactate - targeted resuscitation strategy may be associated with higher mortality in patients with septic shock and normal capillary refill time : a post hoc analysis of the ANDROMEDA - SHOCK study. Ann Intensive Care 10:114.
13. Hernandez G, Carmona P, Ait-Oufella H. Monitoring capillary refill time in septic shock.Intensive Care Med. 2024;50(4):580-582. doi:10.1007/s00134-024-07361-3.
14. Kleinman ME, Chameides L, Schexnayder SM, et al. Pediatric advanced life support: 2010 American Heart Association Guidelines for Cardiopulmonary Resuscitation and Emergency Cardiovascular Care. Pediatrics. 2010;126(5):e1361-e1399.
15. Reinhart K, Daniels R, Kissoon N, Machado FR, Schachter RD, Finfer S. Recognizing Sepsis as a Global Health Priority - A WHO Resolution[J]. N Engl J Med. 2017;377(5):414-417.
16. Fernández-Sarmiento J, De Souza D, Jabornisky R,et al. Paediatric inflammatory multisystem syndrome temporally associated with COVID-19 (PIMS-TS): a narrative review and the viewpoint of the Latin American Society of Pediatric Intensive Care (SLACIP) Sepsis Committee[J]. BMJ Paediatr Open. 2021;5(1):e000894. Published 2021 Feb 4.
17. Huber W, Zanner R, Schneider G, et al.. Assessment of Regional Perfusion and Organ Function: Less and Non-invasive Techniques[J]. Front Med (Lausanne). 2019;6:50. Published 2019 Mar 22.
18. Mosorov V.The Lambert-Beer law in time domain form and its application[J].Appl Radiat Isot,2017,10(128):1-5.

 doi:10.20944/preprints202411.0568.v1

disclaim responsibility for any injury to people or property resulting from any ideas, methods, instructions or products referred to in the content.